Supplementary figure S1

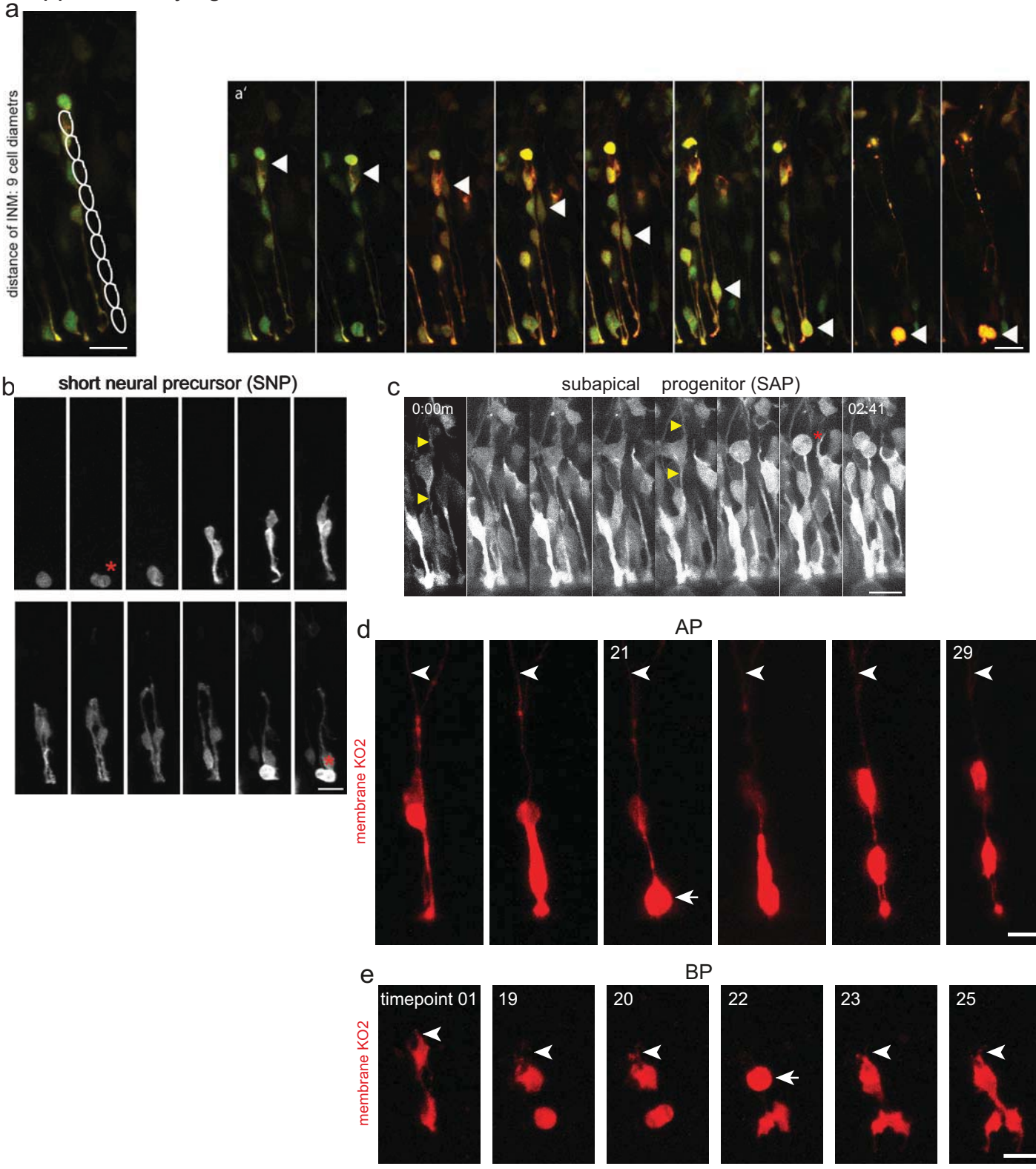

The extent of interkinetic nuclear migration in the LGE defining VZ and SNP/SAP progenitor subtypes extracted from imaging
(a) Example of soma positions (white circles) of a radial glia cell undergoing interkinetic nuclear migration towards the ventricle. White circles in a illustrate the distance travelled as a measure of cell diameters. INM was observed during live imaging in slices. (Single time-lapse pictures of a are depicted in (a'), time-frame is 20min. Note that interkinetic nuclear migration comprises between 8-11 cell diameters, which was used as definition for the ventricular zone thickness. (b) Single timeframes taken from a slice imaging experiment depicting a short neural precursor dividing two times (red asterix). Notably, after the first division, 2 SNP daughter cells are generated (time frame 20min; different timepoints selected, time difference not equal). (c) Images of a bipolar, RG like SAP, that divides in sub-apical position (yellow arrowheads point to apical and basal processes; red asterix marks the cells in m-phase). (d,e) Examples of an AP and BP labeled with a membrane bound form of Kasabian orange (arrows point at cells in M-phase, arrowheads to labeled processes of the cells). Scale bars (a-e): 20µm.

Supplementary figure S2

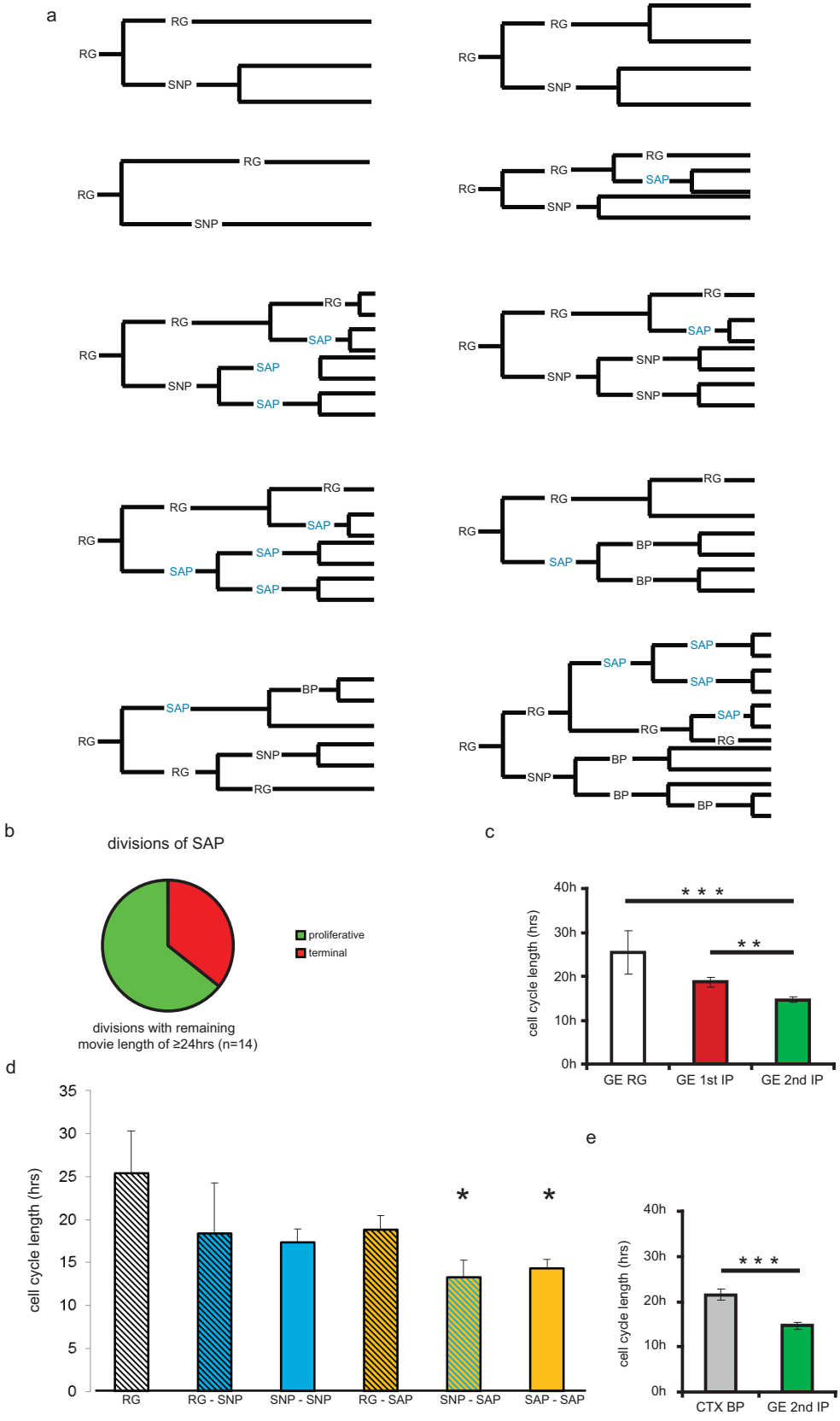

Lineage trees obtained from live imaging show abundance of SAPs in larger clones and cell cycle analysis of divisions in the LGE and cerebral cortex

(a) Exemplary lineage trees obtained from 3 different experiments with the duration of imaging ranging from 47-49hrs. SAPs are highlighted in blue. Note that SAPs are particularly abundant in larger lineages of >4 cells and can be generated by RGs, SNPs and also SAPs. (b) Percentage of proliferative and terminally differentiating SAPs (analyzed when at least 24hrs of movie remained after last SAP division; n=14). (c) Histogram depicting the cell cycle length in hours of subsequent divisions of LGE progenitors determined from time-lapse movies. Note the gradual shortening during subsequent divisions with 2nd intermediate progenitor (IP) divisions showing a significantly shorter cell cycle than RG (p=0.0015; t-test) and first generation IP (generated from RG; p=0.0039; t-test; n=6, 10, 18, respectively; error bars are s.e.m.). (d) Histogram of cell cycle length in regard to the origin of each progenitor class (mother cell is named first). Stars indicate significant difference to cell cycle length of RGs (p=0,05; t-test; RG n=6; RG-SNP n=3; SNP-SNP n=4; RG-SAP n=7; SNP-SAP n=6; SAP-SAP n=8; error bars are s.e.m.) (e) Histogram of cell cycle length comparing the 2nd intermediate progenitor divisions in the LGE to the cell cycle length of BPs in the cerebral cortex revealing a significantly shorted cell cycle of the former compared to the latter (p=0.0001; t-test; GE 2nd generation IPs n=18; CTX BP n=23; error bars are s.e.m.).

Supplementary figure S3

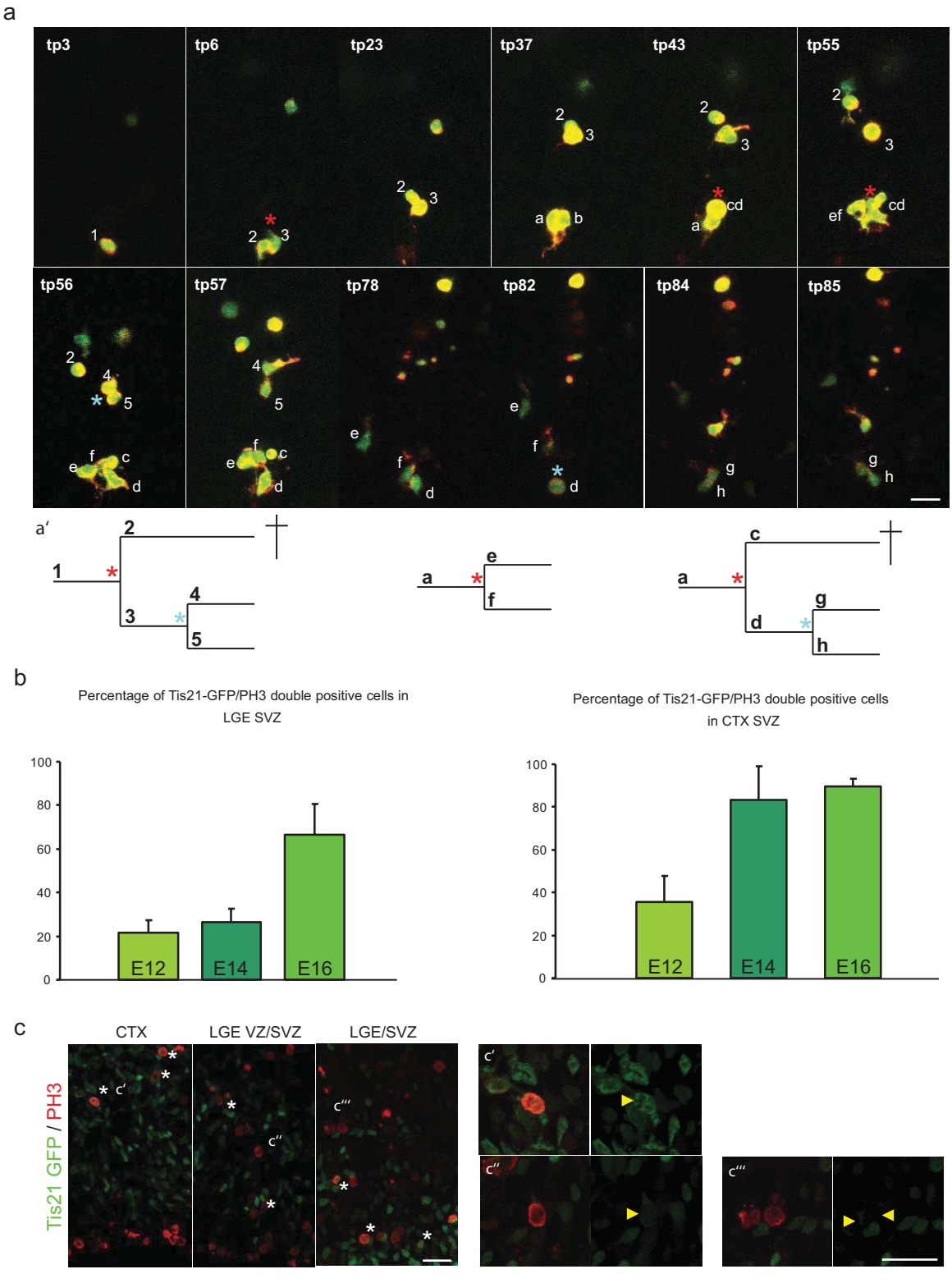

Basal progenitors continue to proliferate in the LGE

(a) Time-lapse series of a basal progenitor (labeled 1) located deep in the SVZ of the LGE that divides at time point 6 (tp6; red star) giving rise to daughter cells 2 and 3 with daughter 3 dividing again (tp56; blue star) to generate cells 4 and 5. Cell b also divides (tp43; red star) generating daughter cells c and d of which cell d divides one more time (tp82; blue star) giving rise to daughter cells g and h. One time frame is 20 minutes. (a') Schemes illustrating the cells tracked in (a) stars indicate divisions of BPs (red=1st, blue= 2nd). Note that the drawing is not to scale. Scale bar (all pictures in a): 20µm. (b) Quantification of Tis21::GFP positive non-apically dividing progenitors in LGE and cerebral cortex from E12 to E16 (error bars are s.d.) (c) Fluorescence micrographs of PH3 staining (red) in Tis21::GFP (green) mice show examples of double-positive progenitors in the cerebral cortex (white asterisks). Inserts c' c'' depict double positive cells and in (c''') Tis21-GFP negative cells indicated by yellow arrowheads. Scale bar (all pictures in c, c'-c''' 30µm).

Supplementary figure S4

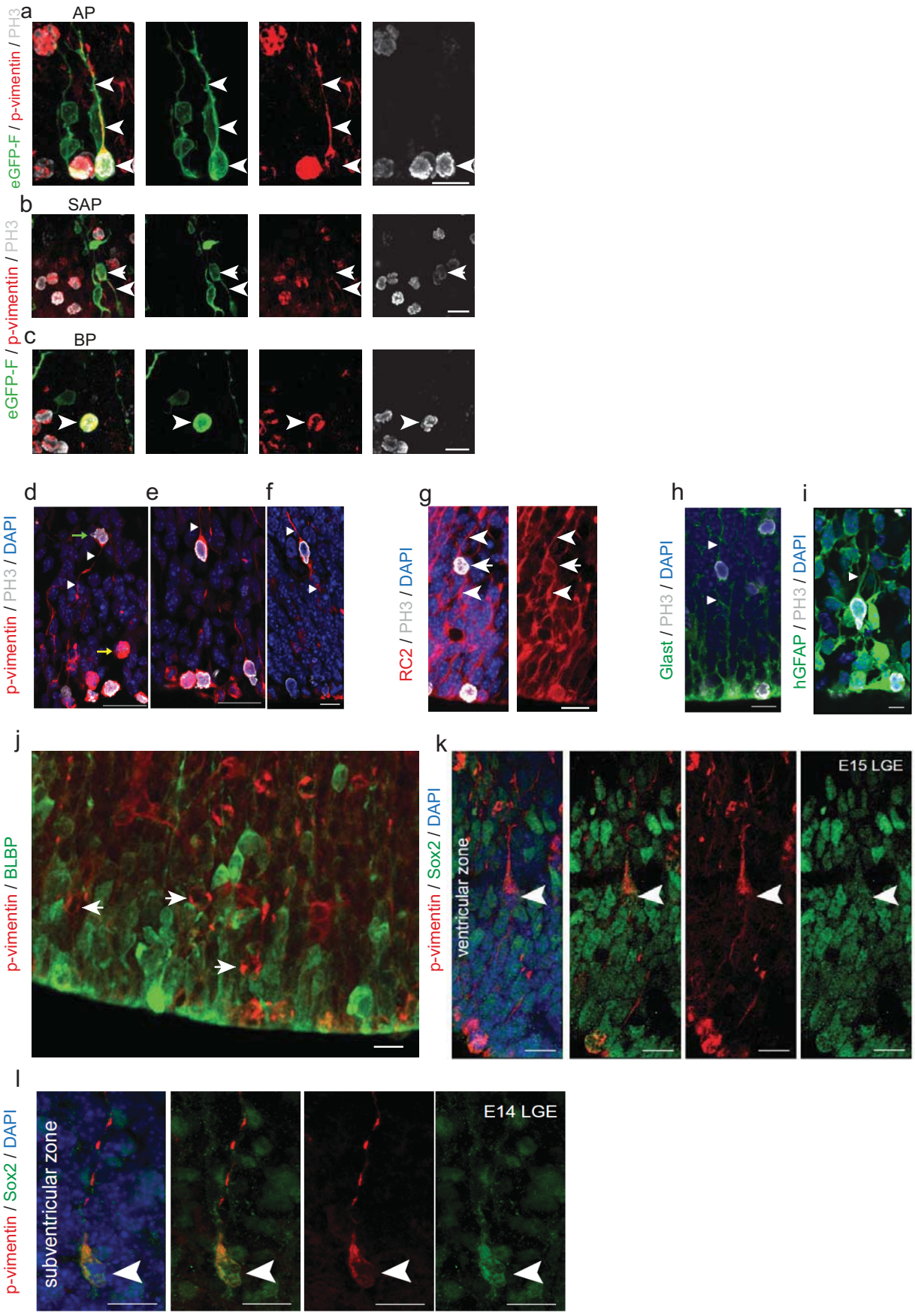

Phospho-vimentin reliably labels cellular processes in M-phase and a part of the heterogeneous population of SAPs shows bipolar morphology and expresses RG specific molecules

(a-c) Examples of an AP, SAP and BP showing co-labeling of membrane bound GFP (eGFP-F; green) and p-vimenin (red; arrows point to cell body in M-phase; arrowheads to cellular processes in a,b) see also 3D reconstructions in Supplementary movie S8; (d-f) Fluorescence micrographs of E14 mouse telencephalon sections immunostained for mitotic cells by phosphorylated histone H3 (PH3) and phosphorylated vimentin (p-vimentin). White arrowheads point at apical (d,f) or basal (e,f) processes of mitotic cells. Note SNP like (green arrow in d) and multipolar cells (yellow arrow in d) dividing in the LGE VZ. (g-i) SAPs express radial glia markers Nestin/RC2 (g) Glast (h) and hGFAP (i). Sub-apical RGs in the VZ and bRG in the SVZ of the LGE also stain positive for Sox2 (white arrowhead in j and k). Scale bars: 20µm (a-g, h,j), 10µm (i).

Supplementary Figure S5

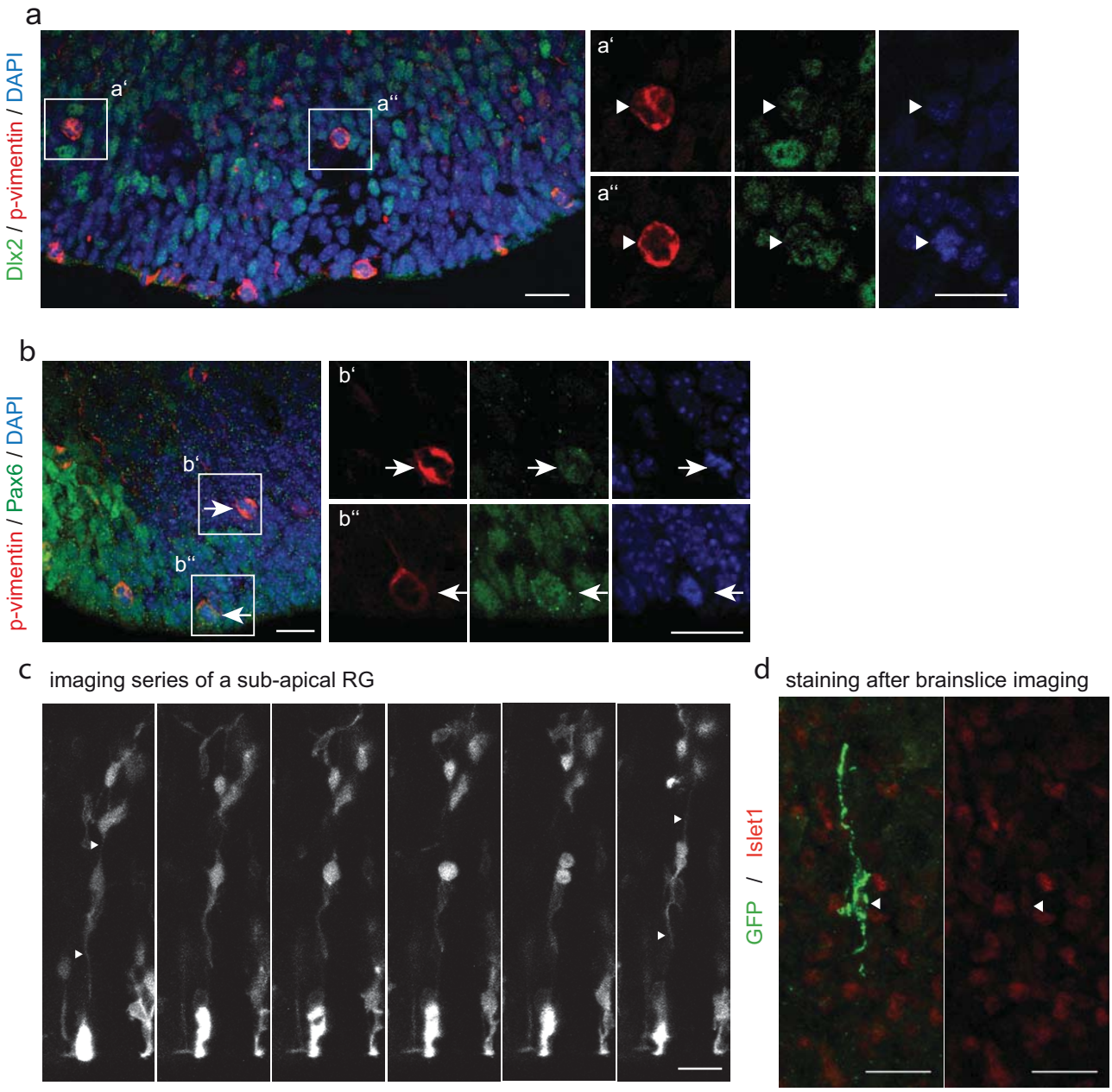

SAPs express Dlx2 and Pax6 transcription factors – sub-apical RG give rise to bRG and Islet1+ neurons
(a,b) Fluorescence micrographs of E14 mouse telencephalon showing the expression of Dlx2 and Pax6 in SAPs and APs of the LGE (boxed panels in a',a'',b' and b'' show a single optical section; arrowhead pointing at mitotic cell). (c) Time-lapse series of a sub-apically dividing RG. White arrowheads point at apical and basal processes. The two daughter cells relocated in the fixed and stained (GFP/green, Islet1/red) slice after 48hrs of imaging. (d) Fluorescence micrograph shows weak expression of Islet1 (white arrowhead) in the more apical located daughter cell. Also in other species the more apical daughter cell is destined to differentiate into a neuron (refrence 40). Scale bars (a-d): 20µm.

Supplementary figure S6

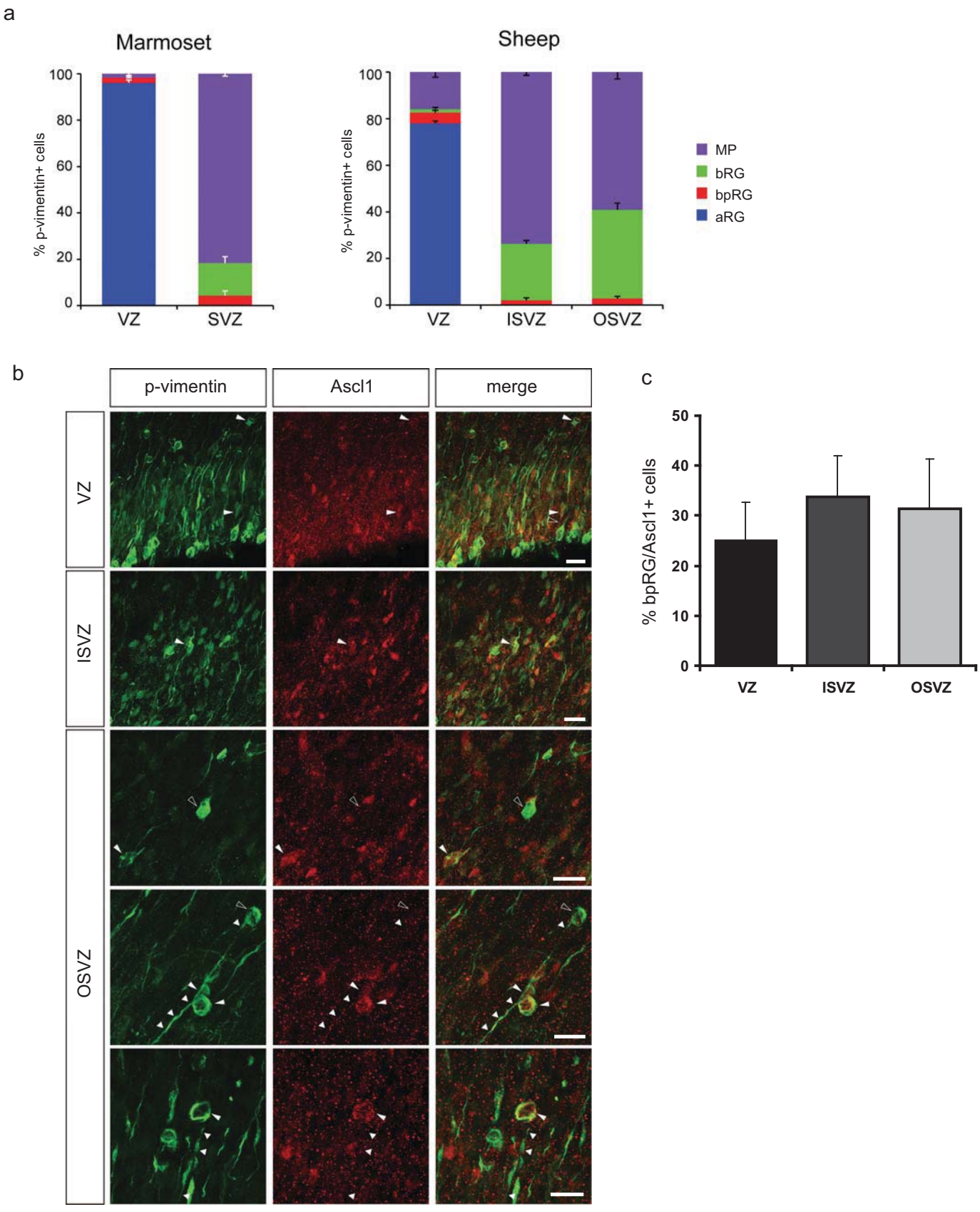

Progenitor subtypes determined by phosphorylated vimentin immunostaining in the developing neocortex of marmoset and sheep embryos
(a) Histograms depict proportions of aRG, bpRG, bRG and MPs within the VZ, SVZ, ISVZ or OSVZ of the neocortex of marmoset (E85) and sheep (E65-67) embryos, as defined by p-vimentin stain (marmoset, n = 1581 cells in VZ, 162 cells in ISVZ; sheep, n = 563 cells in VZ, 932 cells in ISVZ, 940 cells in OSVZ; 3 embryos each). Data are mean +/- S.E.M. (b) Fluorescence micrographs showing the co-labeling of dividing bpRG (p-vimentin; green) with Ascl1 (red) in the VZ, ISVZ and OSVZ of the ferret (P2). Long white arrowheads indicate Ascl1+ cells, empty arrowheads Ascl1- cells, and small white arrowheads point to processes of dividing cells. All scale bars in b: 20μm (c) Quantification of bipolar p-vimentin/Ascl1+ double positive cells in the VZ (n=114), ISVZ (n=90) and OSVZ (n=95) of the ferret cortex (P2) (Error bars are s.e.m).

Supplementary figure S7

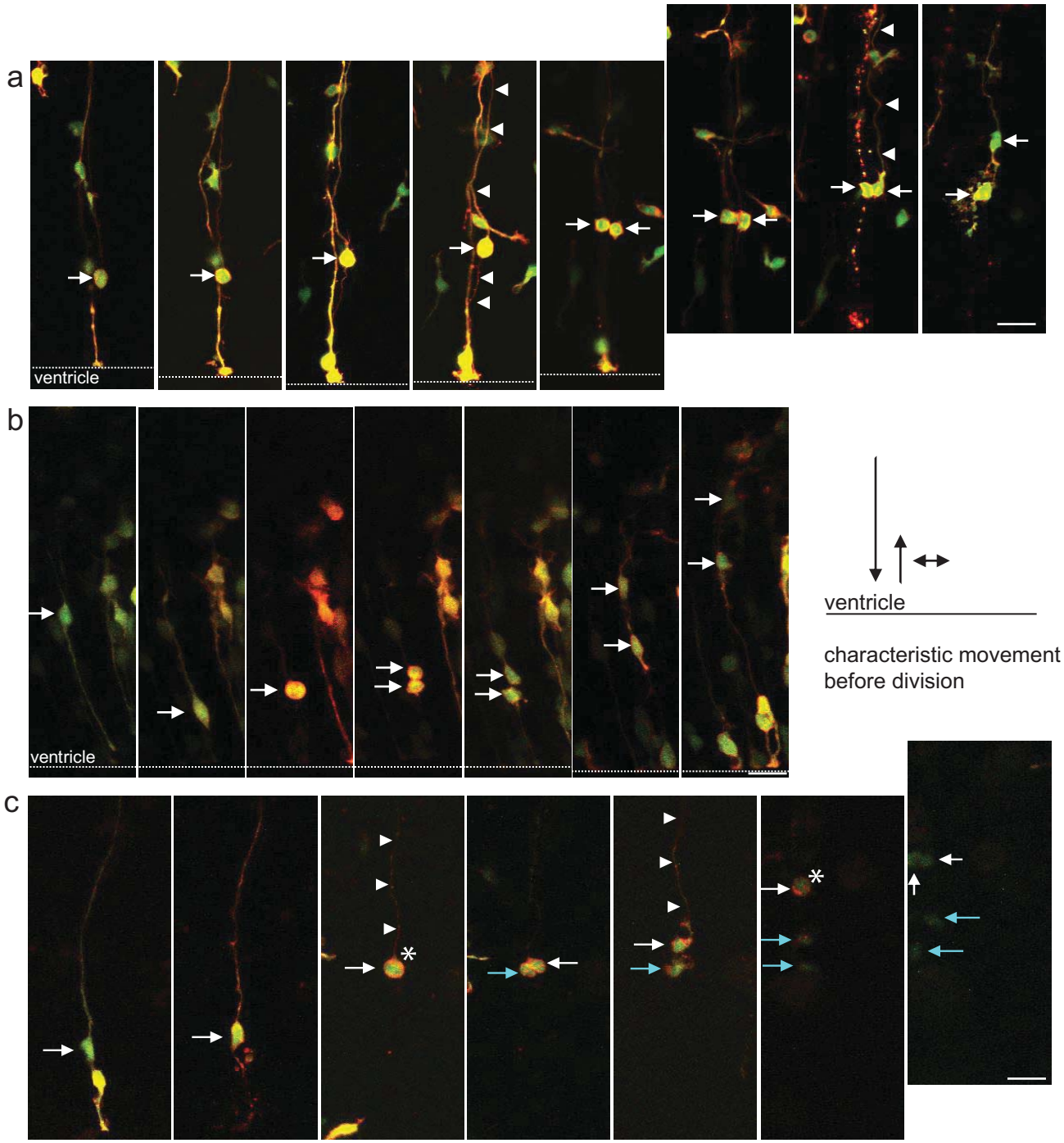

Interkinetic nuclear migration of sub-apical progenitors and basal radial glia
(a) Example of an SAP (white arrow) dividing in the VZ retaining apical and basal processes (white arrowheads). One daughter cell inherits the basal process (white arrowheads) and starts to trans-locate basally, maintaining the basal process reminiscent of basal radial glia (bRG). (b) Characteristic movement of a RG-like SAP soma before division at sub-apical position. The soma moves apically, but before reaching the apical surface returns basally to divide at a sub-apical position (white arrows). The two daughter cells with bipolar morphology move basally. (c) Time lapse series of a bRG (white arrow) originating apically moving basally and dividing twice (white stars). The daughter cell after the first division (blue arrow) divides once more with a shorter cell cycle than the bRG mother cell. Scale bars (a-c): 20µm.

Supplementary figure S8

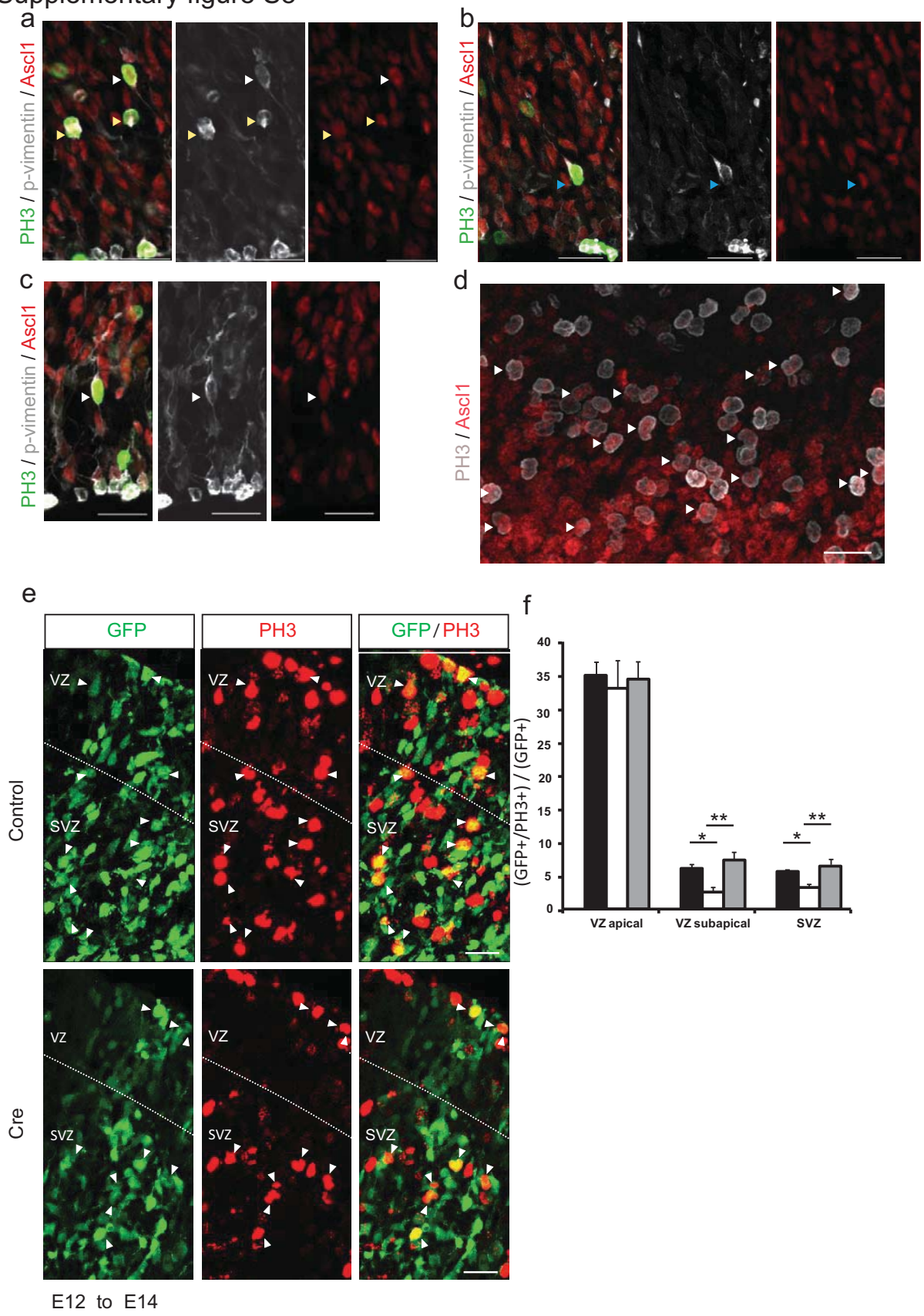

Deletion of the transcription factor Ascl1 reduces the number of SAP and BP in E14 LGE

(a-c) Fluorescence micrographs depicting SNP-like (white arrow in a; only apically directed process), multipolar (yellow arrows in (a)), bRG (green arrow in (b); only basally directed process) and RG-like (white arrow in (c); apical and basal process) SAPs positive for Ascl1. (PH3, green; p-vimentin grey; Ascl1, red). (d) Dividing BPs (PH3; grey) in the SVZ of E14 LGE; BPs positive for Ascl1 (red) are highlighted by white arrowheads; Scale bar: 20µm (e) Fluorescence micrographs of LGE at E14 after electroporation of Cre-GFP together with GFP-control or GFP-control plasmid only into Ascl1flox/flox mice (e) or electroporation of Cre-GFP into Ascl1flox/+ mice (data not shown) at E12. The number of dividing cells in both VZ and SVZ is reduced after electroporation of Cre (note white arrowheads indicating Cre-GFP/PH3 double positive cells; the border between VZ and SVZ is marked by a dashed white line). (f) Quantification of GFP/PH3 double positive cells in apical, VZ/sub-apical and SVZ position after electroporation of GFP-control plasmid or Cre-GFP into the LGE of Ascl1 flox/flox or Ascl1 flox/+ control animals (n=6 animals; VZ sub-apical: * $p<0.05$; SVZ: ** $p<0.01$; student's t-test; error bars are s.e.m.). After knockout of Ascl1 the numbers of cells dividing in VZ/sub-apical or SVZ are reduced, whereas the numbers of apically dividing cells are unchanged. Scale bar (a-c): 20µm.

Supplementary figure S9

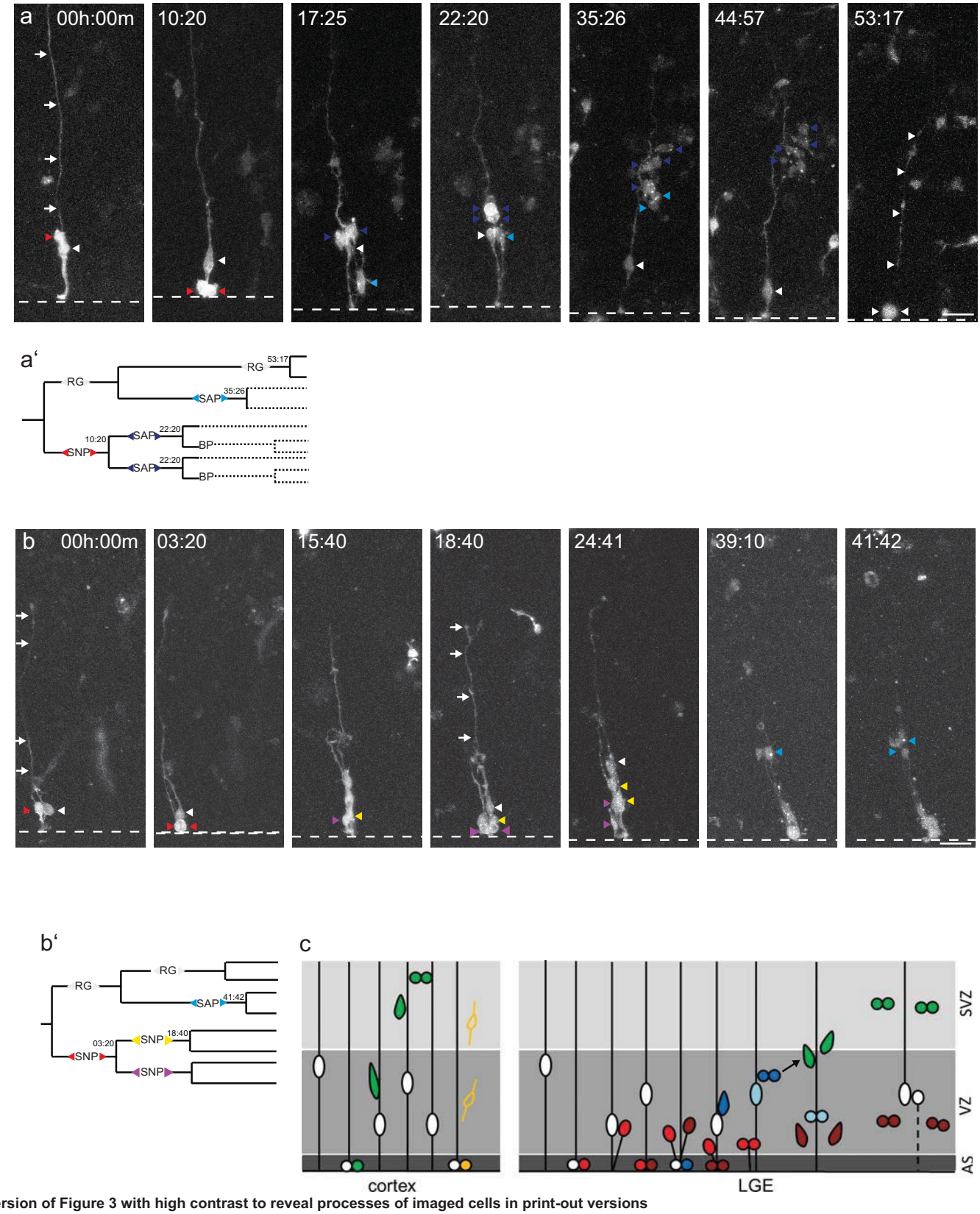

Version of Figure 3 with high contrast to reveal processes of imaged cells in print-out versions

(a) Time-lapse series of a clone consisting of a RG (white arrowhead) and a short neural progenitor (SNP, lacking a basal process, red arrowhead). The SNP divides at the ventricle (dashed white line) (t: 10:20) giving rise to two SAPs (dark blue arrowheads) that divide again in the VZ (t:22:20). The radial glia cell also divides at the ventricle giving rise to a RG and a sub-apically dividing progenitor (SAP, white and blue arrowhead in t:17:25). The SAP divides in the VZ (two blue arrowheads in t:35:26), whereas the RG undergoes mitosis at the ventricle (t:53:17). White arrowheads point at the RGs basal process (t:00:00 and t:53:17). (a') Lineage diagram derived from the time-lapse movie in (a), note that BPs continued to proliferate in the SVZ, but could not be individually followed due to their fast movement and decreased GFP-signal (dashed lines). Note that the length of the lines in (a') and (b') are not drawn to scale (time). Scale bars 20µm (b) Time-lapse series illustrating the generation of multiple VZ progenitors coming from a single labeled cell. The SNP divides at the ventricle (red arrowheads; t:03:20), giving rise to two SNPs that divide again at the ventricle (red arrowheads at t:18:40). The RG (white arrowhead in t:03:20) gives rise to one RG and one SAP that is dividing between t:39:10 and t: 41:42 (blue arrowheads). (b') Lineage diagram derived from the time-lapse series in (b). Note that the two daughter SNPs generated by a SNP (red) divide at a very similar time point at the ventricle. Scale bar: 20µm. (c) Scheme illustrating the progenitor lineage detected in the LGE in comparison to the neocortex. In the developing cortex at midneurogenesis RG divide mostly asymmetrically to give rise to either neurons (yellow) or BPs (green) that migrate to divide in the SVZ. In the LGE RG cells generate progenitor cells that continue to proliferate in the VZ either as SNPs (red) or SAPs (blue). SNPs and SAPs can perform self-renewing divisions in the VZ thereby amplifying the progenitor pool. Sub-apically dividing radial glia also divide in the VZ and sometimes generate a daughter cell with bRG morphology.